Analysis of Real Overvoltage Disturbances by Using Nonstationary Signal Processing Techniques

Snežana VUJOŠEVIĆ, Saša MUJOVIĆ, Miloš DAKOVIĆ
University of Montenegro, Faculty of Electrical Engineering, 81000 Podgorica, Montenegro
sasam@ac.me

***Abstract*—Switching surges can cause voltage conditions degradation, and this paper presents a new approach in their analysis. Besides the amplitude properties, regarding to power quality, it is important to know the structure of their harmonic spectrum. For that purpose, characteristic surges (energization and deenergization of an unloaded 35 kV underground cable, energization of an unloaded 10 kV underground cable and deenergization of a 10 kV overhead line, with a multiple appearance of the arc between the circuit breaker contacts) were analyzed. The signals were obtained by an experiment, so the occurrence of noise makes them much more complex to analyze than the simulated ones. Their harmonic decomposition was performed by digital signal processing methods - Empirical Mode Decomposition and Short Time Fourier Transform. The obtained results were compared to the calculated ones, which allowed us to draw conclusions related to applied methods efficiency and characteristic harmonics values that occur during the switching surges. The performed analysis allows us to get a deeper insight into transient processes in the real transmission power lines. The obtained results can be especially useful to detect the locations of occurrence of various types of surges and for development of real-time power quality monitoring systems.**

***Index Terms*—empirical mode decomposition method, harmonics, power quality, short time Fourier transform, switching surges.**

I. Introduction

In modern distribution systems power quality is almost as important for suppliers as it is for consumers of electric energy. Voltage sags and dips, the appearance of harmonics, overload of transformers, significant neutral line currents and strong overheating of the lines are the typical problems related to a poor voltage supply quality [1], [2]. Detection of the above mentioned problems is the first step in their elimination [3], [4].

In this paper, a special attention is devoted to the switching overvoltages caused by the rapid changes of the electrical circuits working regime (i.e. switching commutations) and to their impact on the voltage supply quality. The overvoltages are a specific type of problem, with a short duration and non-periodic waveform, which consequently require a special type of analysis. Their occurrence may cause damage to the insulation or some parts of the equipment and also degradation of power quality. Therefore, it is necessary to identify and eliminate their effects [5].

So far, common approach in the switching surges analysis was based on consideration of the surge waveform maximum value. In other words, the values of frequencies and harmonics that accompany the observed process were not taken into account [6-11]. From today's point of view, bearing in mind a dramatic increase of sensitive electronic devices in the load profile of modern systems and the importance of power quality, such an approach is unacceptable. In order to overcome the foregoing constraint, digital signal processing methods are increasingly used in analyzing switching surges and power quality disturbances [12-21]. Probably, our first thought regarding above mentioned may be connected with application of Discrete Fourier Transform (DFT) as a well-known method [22]. However, the method is convenient only for periodical and stationary signals. As previously mentioned, switching surges have completely different characteristics and the DFT method is not appropriate for their analysis [23, 24]. In connection with this, this paper promotes the Empirical Mode Decomposition (EMD) method, which is convenient for the nonlinear and nonstationary data analysis. The main innovation of the method is the introduction of intrinsic mode functions based on the local properties of the signal [12-15], [25, 26]. In the above referenced papers the EMD method was applied only to the theoretical signals, which are the result of more or less accurate simulations. This fact inspired us to check adequacy of the model for analysis, i.e. decomposition, of real surge signals into component frequencies. It should be emphasized that real signals are accompanied by noise, which makes the analysis more complex. To that end, measurements were carried out and time presentations of four characteristic switching surges were recorded: energization of an unloaded 35 kV underground transmission cable, deenergization of the unloaded 35 kV underground cable, energization of an unloaded 10 kV underground transmission cable and deenergization of a 10 kV overhead transmission line.

Besides using the EMD method, the analysis of these signals was performed by Short Time Fourier Transform (STFT) method, which is a standard transformation for signals with time-varying spectrum analysis [22]. The results obtained by the EMD and STFT methods were compared with calculated ones and conclusions related to their efficiency and characteristic harmonics bands that occur in the analyzed types of switching surges were drawn. Availability of data regarding the structure of the harmonic spectrum allows more detailed insight into the observed transient processes and associated phenomena.

Digital Object Identifier 10.4316/AECE.2015.03004

II. BACKGROUND

This section discusses methods for analytic determination of frequencies that occur as a result of switching surges and gives an overview of digital signal processing methods EMD and STFT, which are used in the examples that correspond to the transient occurrences analyzed later in the paper.

A. Analytical determination of the expected frequencies

The analysis of measured voltage signals waveform is very important from the power quality point of view, because they represent the observed process in the most realistic way. In the case of switching surges, the analyzed signals are signals with fast changing spectral contents. Therefore, it is very important to choose a convenient method for the analysis and to verify its accuracy and efficiency. This can be done by comparing the results obtained by digital signal processing methods with analytically calculated values.

For analytical determination of frequencies that appear during the switching surges the transient process is considered as nonsymmetrical and the analysis is performed using the method of symmetrical components. During the process of energization and deenergization of three-phase overhead transmission lines and underground cables, the traveling waves propagate along the line and their refraction and reflection occurs. The time in which the surge wave arrives from the beginning to the end of line is:

$$\tau = l \cdot \sqrt{L \cdot C} \tag{1}$$

for direct component, and:

$$\tau_0 = l \cdot \sqrt{L_0 \cdot C_0} \tag{2}$$

for zero component, where l is the length of the line, whereas L, L_0, C, C_0 are lines inductances and capacitances per unit length, for direct and zero sequence respectively.

The velocities of the wave's propagation along the line are:

$$v = 1/\sqrt{L \cdot C} \tag{3}$$

and

$$v_0 = 1/\sqrt{L_0 \cdot C_0} \tag{4}$$

It is well known that, for the overhead transmission lines, the propagation velocity of the direct component of the traveling waves is very close to the speed of light, whereas it is considerably lower for the underground cables. Periods of the corresponding components of the switching surge are 4τ and $4\tau_0$ respectively. In the three-phase presentation, the following frequency values are calculated:

- The refraction and reflection of the traveling waves (direct component) with velocity value v along the unloaded transmission line with length l causes the frequency value:
$$f = v/(4 \cdot l) \tag{5}$$
- The refraction and reflection of the traveling waves (zero component) with velocity value v_0 along the unloaded transmission line with length l causes the frequency value:
$$f = v_0/(4 \cdot l) \tag{6}$$
- The transition of the system from one stationary state to another causes natural frequencies of the system (direct and zero component), which can be calculated based on the equivalent line T scheme:
$$f = 1/\left(2 \cdot \pi \sqrt{(L_e + L \cdot l/2) \cdot C \cdot l}\right) \tag{7}$$
$$f = 1/\left(2 \cdot \pi \sqrt{(L_{e0} + L_0 \cdot l/2) \cdot C_0 \cdot l}\right) \tag{8}$$

where L_e is equivalent generator and transformer inductance.

From the equations 1-8 follows that the accuracy of the results obtained analytically depends on the knowledge of the input data for L and C, which are not always readily available, and this makes the application more complex.

B. Empirical Mode Decomposition

The EMD is a novel signal analysis tool which gives sharp identification of embedded signal components. It was introduced by N. E. Huang [12] and it has become an important tool for signal decomposition and analysis. Recently, EMD has been successfully applied to power quality monitoring [13], power line energization [14], as well as general signal decomposition [22] and radar signal processing problems [26].

The EMD decomposes a given signal $x(t)$ into a sum of intrinsic mode functions (IMF) through an iterative process called *sifting*. By definition, an IMF satisfies two conditions:

1. The number of extrema and the number of zero crossings may differ by no more than one.
2. The average value of the envelope defined by the local maxima, and the envelope defined by the local minima, is zero.

Thus, locally, each IMF contains lower frequency oscillations than the previously extracted one. The IMFs are obtained using the following algorithm (sifting process) [22], [26]:

1) Identify all extrema of $x(t)$.
2) Interpolate between minima (maxima) obtaining envelopes $e_{low}(t)$ (resp. $e_{up}(t)$).
3) Compute the average envelope $m(t) = \left(e_{up}(t) + e_{low}(t)\right)/2$.
4) Extract the detail $d(t) = x(t) - m(t)$.
5) If $d(t)$ is an IMF, extract it and replace $x(t)$ with $r(t) = x(t) - d(t)$, if $d(t)$ is not an IMF, continue *sifting* replacing $x(t)$ with $d(t)$.
6) Repeat steps (1) – (5) until some of the stopping criteria are satisfied.

To guarantee that the IMF functions retain enough physical sense, we have to determine criterion for the sifting process to stop. The most widely used criterion is to limit the size of standard deviation (SD), computed from the two consecutive sifting results as:

$$SD = \sum_{t=0}^{T} \left[\frac{\left| imf_{(k-1)}(t) - imf_k(t) \right|^2}{imf_{(k-1)}^2(t)} \right] \tag{9}$$

The sifting stops when SD value comes between 0.2 and 0.3 (experimentally determined threshold). By summing all IMF components with residual we obtain:

$$x(t) = \sum_{i=1}^{N} imf_i + r_N \tag{10}$$

Thus, we achieved a decomposition of the data into N

empirical modes, and a residue r_N, which can be either the mean trend or a constant.

In order to present EMD, as well as method's applicability for switching surges analysis, a simulation of energization of unloaded 35 kV line in a single phase ground fault was considered. The signal in time domain, for phases that are not in a ground fault, is presented in Fig.1. It should be emphasized that the signal is not symmetrical, which is quite common case in engineering practice.

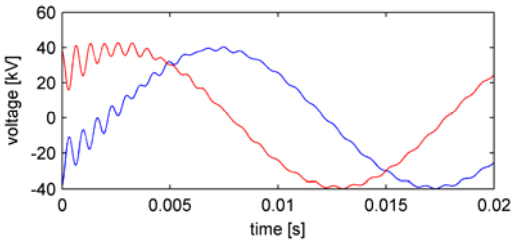

Figure1. Energization of unloaded 35 kV overhead transmission line in a single phase ground fault (simulation results)

The line length is l=7.5 km, and a characteristic impedance is Z_c=370 Ω. With the application of an analytical approach on considered signal, frequency values of f_1= 50 Hz, f_2= 1170.285 Hz and f_3= 1526.755 Hz were obtained. Results of decomposition (IMFs) are presented in Fig. 2, while Fig. 3 depicts IMFs in frequency domain.

The signal is sampled with $\Delta t = 2\times10^{-5}$s and 1000 signal samples are used as input to the EMD.

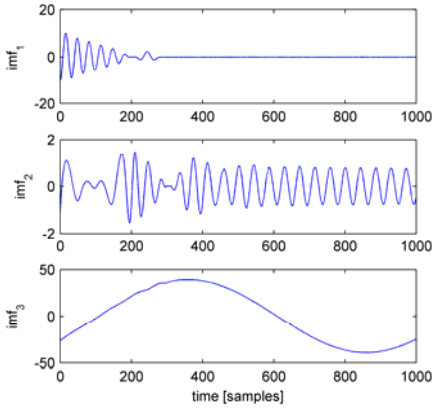

Figure 2. Energization of unloaded 35 kV overhead transmission line in a single phase ground fault. Obtained IMFs for signal presented in Figure 1.

Fig. 3 illustrates Fourier transform of the IMFs. It can be seen that EMD successfully decomposes the signal into individual components. Here we can stop searching for IMFs when all components of interest are obtained. In real application we either should know the number of components *apriori* or we should stop decomposition when residue does not contain components of interest. Estimated frequencies from the individual IMFs are f_1= 50.35 Hz, f_2= 1167.29 Hz and f_3= 1525.87 Hz. They are very close to the exact frequencies.

Further analysis of the EMD applicability for switching surges is conducted throughout simulation of energization of a very long and unloaded 110 kV overhead line (l=500 km and Z_c=273 Ω). The analyzed process is symmetrical. The signal, given in Fig. 4, is very close to real one, and beside the fundamental frequency (50 Hz), it contains two transient components at frequencies 92.925 Hz and 336.775 Hz. The decomposition results (IMFs) are presented in Fig. 5, while Fig. 6 illustrates IMFs in frequency domain.

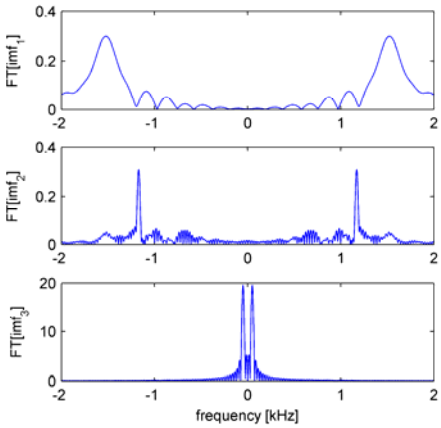

Figure 3. Fourier transform of the IMFs presented in Figure 2. Each IMF contains single component with frequency that correspond to the calculated ones.

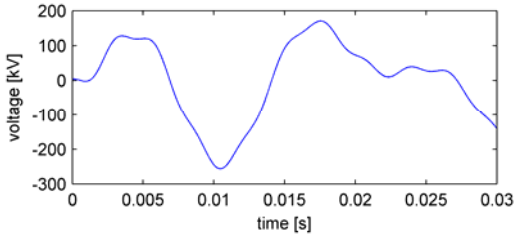

Figure 4. Energization of a very long and unloaded 110 kV overhead transmission line (simulation results)

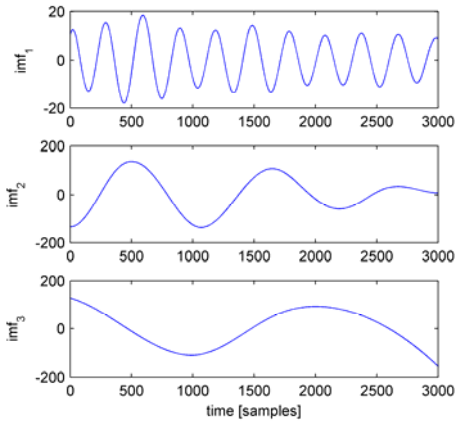

Figure 5. IMFs obtained by EMD for simulated energization of overhead transmission line presented in Figure 4

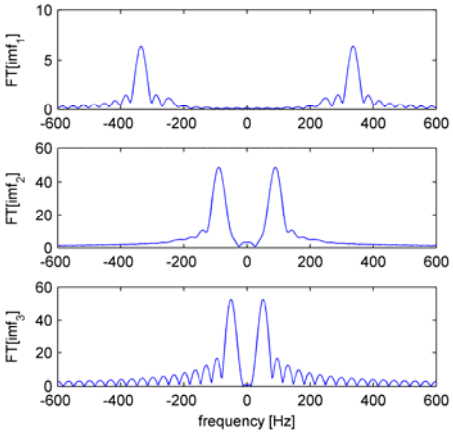

Figure 6. Fourier transform of IMFs from Figure 5. Three signal components are successfully separated.

C. *Short Time Fourier Transform (STFT)*

The STFT is introduced to overcome the problem of

nonstationary signal analysis. It is based on the assumption that for a short-time basis, signal can be considered as stationary. The analytical expression for STFT in continuous time and frequency domain is [22]:

$$STFT(\tau,\omega)=\int x(t)h(t-\tau)e^{-j\omega t}dt \quad (12)$$

The main idea is introducing a sliding window function which will truncate the analyzed signal, and applying the Fourier Transform on the truncated parts. The crucial drawback of this method is that the length of the window is related to the frequency resolution. For any chosen window function the expression $\Delta t \times \Delta f$, where Δt is time and Δf is frequency resolution, is always constant, i.e.:

$$\Delta t \cdot \Delta f \geq \frac{1}{4\pi} \quad (13)$$

Increasing the window length leads to improving frequency resolution, but it means that the nonstationarities occurring during considered interval will be smeared in time. Application of the STFT for the signals given in Fig. 1 and Fig. 4 is presented in Fig. 7 and Fig. 8, respectively.

From the Fig. 7 we can see that all components of interest are well separated in the STFT domain. Also we can see nonstationary (time-varying) component. For the case presented in Fig. 8 two close frequency components could not be separated in the time-frequency domain.

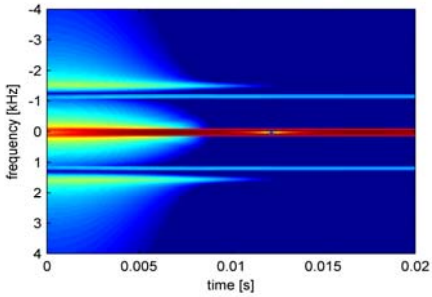

Figure 7. STFT of signal given in Fig. 1. Three frequency components are visible in the STFT domain.

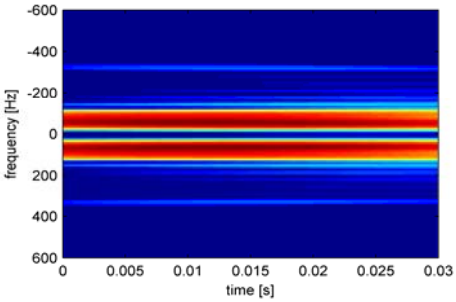

Figure 8. STFT of signal given by Fig. 4. STFT could not separate components located at close frequencies (50 Hz and 92.925 Hz)

III. Description of Measured Overvoltage Signals

For the purposes of this paper, within a study of neutral points grounding for 35 kV and 10 kV distribution networks of the Montenegrin electric power system, measurements were carried out and time presentations of switching overvoltages were recorded. Measurements were carried out in Podgorica on a 35 kV cable line that connects TS 35/10 kV Gorica and TS 35/10 kV Center, on a 10 kV overhead line connecting TS 35/10 kV Gorica and TS 10/0.4 kV Tuzi and on 10 kV underground cable that connects TS 35/10 kV Gorica and TS 10/0.4 kV Zagoric.

The measurements were performed on a single phase, and were carried out by using the following equipment: a capacitive divider for 10 kV voltage level, a multichannel memory oscilloscope, a data acquisition and guidance computer system (DAQ), a specially developed structure for amplification of the command signal of DAQ for the purpose of programming activation (on/off) of a high voltage circuit breaker and a two-channel insulating attenuator for protection of the oscilloscope and DAQ from overflowing of voltage level at their inputs and for adapting amplitudes of the measured signals.

Fig. 9 presents a single-phase model of the analyzed system, where *e(t)* is a time-dependent value of electromotive force; *Re=Rg+Rtr* and *Le=Lg+Ltr* are equivalent generator and transformer resistance and inductance, respectively; *L*, *C,* and *R* are transmission line inductance, capacitance and resistance per unit length.

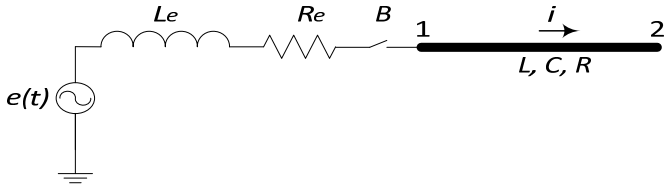

Figure 9. The single-phase model of the analyzed system

The transmission lines with the following characteristics were analyzed:

- A 35 kV underground cable (IPZ013 3x150 mm^2), of a length *l*=2.163 km, and a characteristic impedance. Z_c=34.4 Ω (calculated by equation $Z_c=\sqrt{L/C}$).
- An overhead 10 kV transmission line Al/Fe 3x35 mm^2 of a length *l*=4.8 km and the calculated value of a characteristic impedance Z_c=351 Ω.
- A 10 kV underground cable IP013-A 3x120 mm^2, of a length *l*=5.7 km, and a characteristic impedance Z_c=28.82 Ω.

Voltage signals were obtained at the phase A by an experimental process of unloaded three phase transmission lines energization and deenergization. The measured signals are presented in Figs. 10-13.

Fig. 10 presents the voltage signal, obtained by testing energization of the real unloaded 35 kV underground transmission cable.

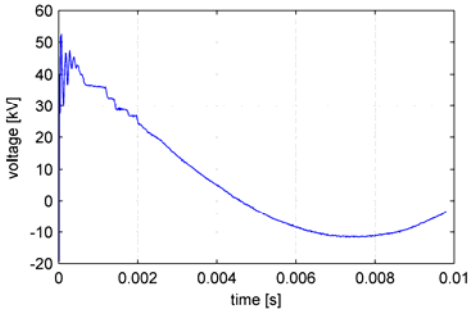

Figure 10. Energization of an unloaded 35 kV underground cable (experimental result)

Fig. 11 presents the voltage signal, obtained by the process of unloaded 35 kV transmission cable deenergization, with a multiple appearance of the arc

between the circuit breaker contacts.

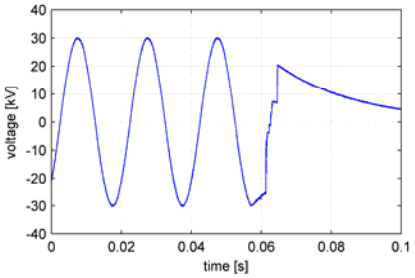

Figure 11. Deenergization of an unloaded 35 kV underground cable (experimental result)

The voltage signal, obtained by experimental deenergization of unloaded 10 kV overhead transmission line, with a multiple appearance of the arc between the circuit breaker contacts, is presented in Fig. 12.

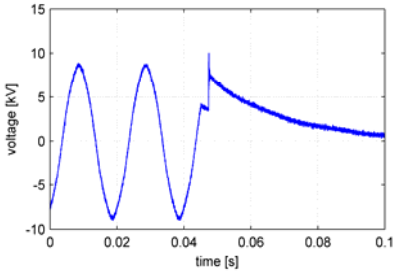

Figure 12. Deenergization of the unloaded 10 kV overhead line (experimental result)

Fig. 13 presents the voltage signal, obtained by testing energization of the real unloaded 10 kV underground transmission cable.

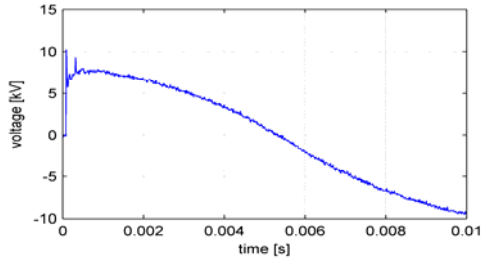

Figure 13. Energization of an unloaded 10 kV underground cable (experimental result)

IV. A Harmonic Analysis of Surges by Implementing EMD and STFT Methods

A. Energization of an unloaded 35 kV underground cable

The voltage signal, presented in Fig. 10, was analyzed by the EMD method in two ways. At first, the signal was analyzed directly, by the EMD method. Then, the 50 Hz sine component and the direct exponential component were removed from the original signal before the analysis in order to provide more accurate values of the extracted frequencies. The reason for the removal of the above components is their very high amplitude in comparison with the amplitude of high frequency components so they could be masked. The voltage signal from Fig. 10, decomposed into intrinsic mode functions, is presented in Fig. 14, whereas Fourier transforms of the obtained IMFs are presented in Fig. 15. The same voltage signal, from which the 50 Hz sine component and the direct exponential component were removed, was also analyzed by the EMD method. Fig. 16 presents the voltage signal, decomposed into intrinsic mode functions. The evaluation of frequencies extracted from the decomposed voltage signal is presented in Fig. 17.

Results obtained by the performed analysis were compared to the frequency values calculated by equations (5)-(8) and presented in Table I. The table is the result of combined application of theory and discussed digital signal processing methods. A mark "-" in the table represents that the marked frequency value was not detected by using the above method.

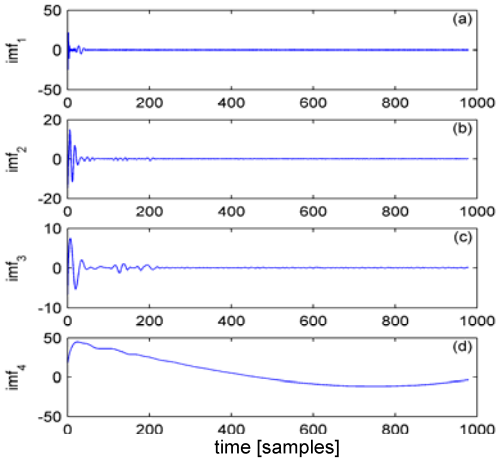

Figure 14. Voltage signal obtained at phase A by energization of the unloaded 35 kV underground cable, decomposed into intrinsic mode functions

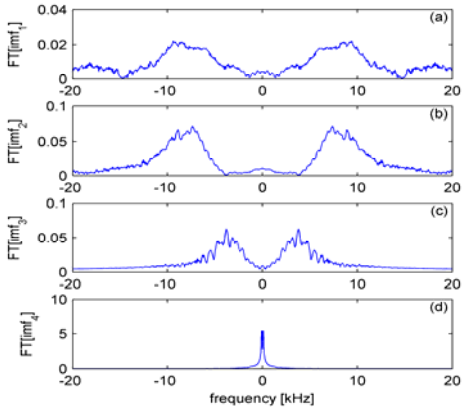

Figure 15. The evaluation of intrinsic mode function frequencies of the voltage signal obtained at phase A by energization of an unloaded 35 kV underground cable

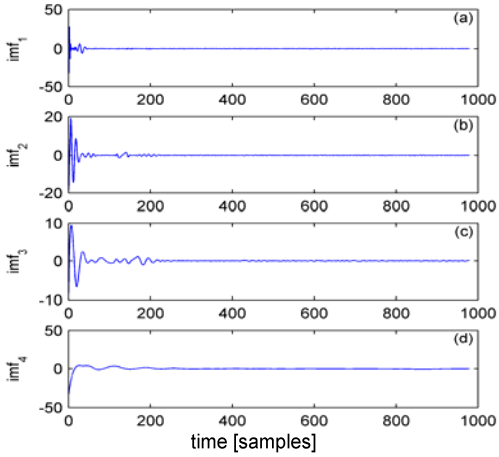

Figure 16. Voltage signal obtained at phase A by energization of the unloaded 35 kV underground cable, decomposed into intrinsic mode functions (after the removal of the 50 Hz sine component and the direct exponential component)

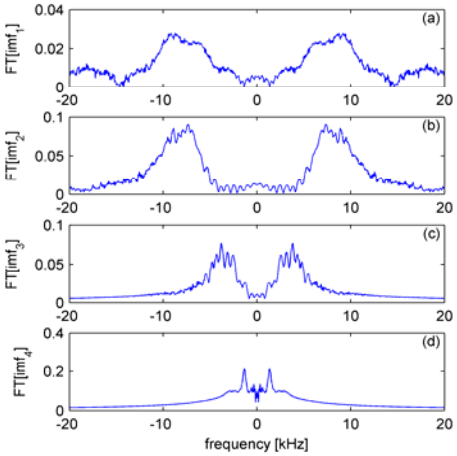

Figure 17. The evaluation of intrinsic mode function frequencies of the voltage signal obtained at phase A by energization of an unloaded 35 kV underground cable (after the removal of the 50 Hz sine component and the direct exponential component)

TABLE I FREQUENCIES OBTAINED BY EMD METHOD: DIRECTLY (EMD1); AFTER THE REMOVAL OF THE 50 HZ SINE COMPONENT AND THE DIRECT EXPONENTIAL COMPONENT (EMD2); COMPARED WITH THE CALCULATED VALUES FOR ENERGIZATION OF UNLOADED 35 KV UNDERGROUND CABLE

Calculated frequency	EMD 1		EMD 2	
	Frequency	Error	Frequency	Error
365 Hz	-	-	341.8 Hz	6.35 %
1286.8 Hz	-	-	1318.3 Hz	2.4 %
3997.4 Hz	3808.8 Hz	4.7 %	3808.5 Hz	4.7 %
9601.7 Hz	9423.8 Hz	1.8 %	9423.8 Hz	1.8 %
	7373 Hz	-	7324.2 Hz	-

The signal was also analyzed by a direct application of the STFT method, and the results are presented in Fig. 18, Fig. 19, and Table II.

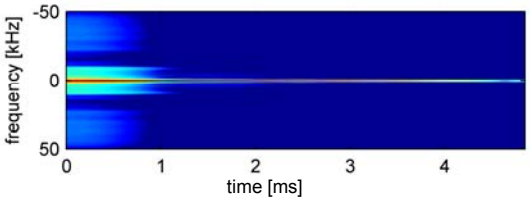

Figure 18. STFT analysis of the voltage signal obtained at phase A by energization of an unloaded 35 kV underground cable

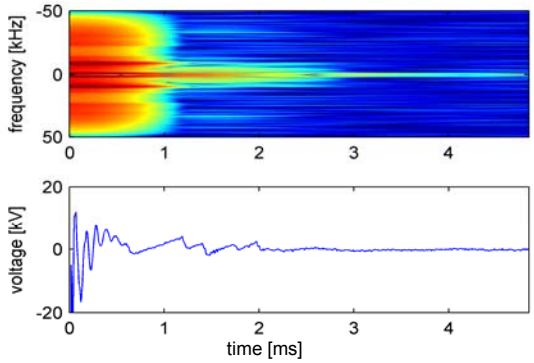

Figure 19. STFT analysis of the voltage signal obtained at phase A by energization of an unloaded 35 kV underground cable (after the removal of the 50 Hz sine component and the direct exponential component)

The comparison between the results of the analysis of the voltage signal obtained by the unloaded 35 kV underground cable energization and the calculated ones shows that results obtained by the EMD method are very close to the calculated values, especially when removal of the 50 Hz sine component and the direct exponential component from the original signal has been performed. In this case, all calculated values of the frequencies are extracted, with the error of 1.8-6.35%. The maximum error value, which corresponds to the minimum expected frequency of 365 Hz, is 6.35%. For the above signal, all of the expected frequency values were extracted by the STFT method, with the error of 5.38-79.45%.

TABLE II FREQUENCIES OBTAINED BY THE STFT METHOD: DIRECTLY (STFT1); AFTER THE REMOVAL OF THE 50 HZ SINE COMPONENT AND THE DIRECT EXPONENTIAL COMPONENT (STFT2); COMPARED WITH THE CALCULATED VALUES FOR ENERGIZATION OF UNLOADED 35 KV UNDERGROUND CABLE

Calculated frequency	STFT 1		STFT 2	
	Frequency	Error	Frequency	Error
365 Hz	521 Hz	42.73 %	655 Hz	79.45 %
1286.8 Hz	1175 Hz	8.68 %	1175 Hz	8.68 %
3997.4 Hz	-	-	3782 Hz	5.38 %
9601.7 Hz	8310 Hz	13.45 %	9005 Hz	6.21 %
	24020 Hz 31580 Hz 36190 Hz	-	24525 Hz 31035 Hz	-

B. Deenergization of the unloaded 35 kV underground cable

The voltage signal, presented in Fig. 11, which was obtained by deenergization of an unloaded 35 kV underground cable, with a multiple appearance of the arc between the circuit breaker contacts, was analyzed by the EMD method. The results are presented in Fig. 20 and Fig. 21. Fig. 20 presents the voltage signal, obtained by deenergization of the unloaded 35 kV underground cable, decomposed into the intrinsic mode functions. Fig. 21 presents the evaluation of frequencies which were extracted from the decomposed voltage signal. The signal was also analyzed by direct application of the STFT method, as it is presented in Fig. 22. The obtained results are presented in Table III.

For the voltage signal obtained by an unloaded 35 kV underground cable deenergization the EMD method gives very accurate results. From four of the calculated values of the frequencies, three are extracted, with the error of 2.93 – 6.68%. For the same signal, by direct application of the STFT method, three frequency values are extracted, with the error of 3.02-8.37%.

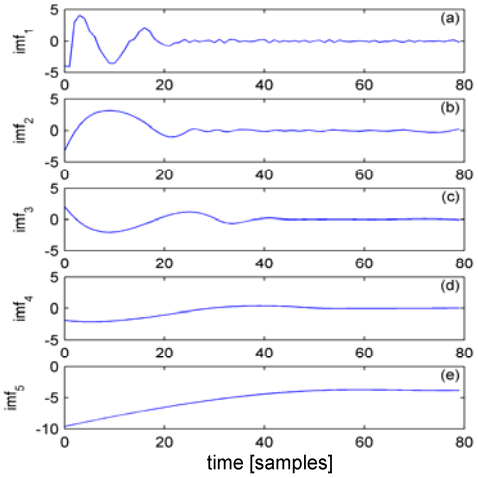

Figure 20. Voltage signal obtained at phase A by deenergization of an unloaded 35 kV underground cable, decomposed into intrinsic mode functions

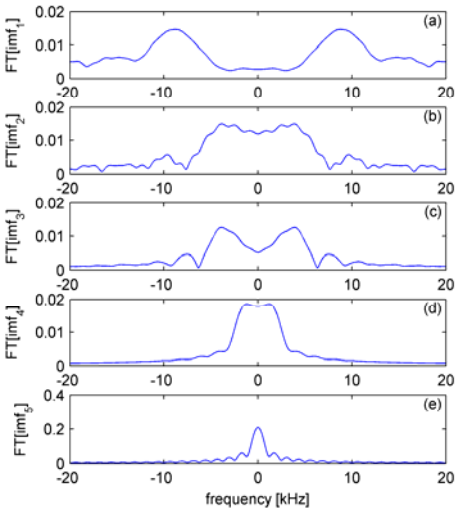

Figure 21. The evaluation of intrinsic mode function frequencies of the voltage signal obtained at phase A by deenergization of an unloaded 35 kV underground cable

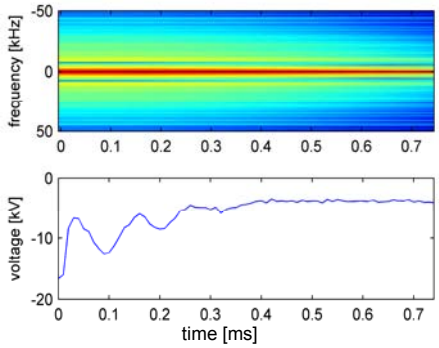

Figure 22. STFT analysis of the voltage signal obtained at phase A by deenergization of an unloaded 35 kV underground cable

TABLE III FREQUENCIES OBTAINED BY THE EMD AND STFT METHODS COMPARED WITH THE CALCULATED VALUES FOR DEENERGIZATION OF UNLOADED 35 KV UNDERGROUND CABLE

Calculated frequency	EMD		STFT	
	Frequency	Error	Frequency	Error
365 Hz	–	–	–	–
1286.8 Hz	1200 Hz	6.68 %	1179 Hz	8.37 %
3997.4 Hz	3877 Hz	3.02 %	4118 Hz	3.02 %
9601.7 Hz	9320 Hz	2.93 %	10052 Hz	4.68 %

Based on the real line parameters, the calculated and extracted frequency values can be explained in the following way:

- the values of natural frequencies for the analyzed system are 1286.8 Hz and 365 Hz. These values were obtained using equations (7) and (8), with the following input parameters: $L = 4.14 \cdot 10^{-4}$ H/km, $C = 0.35 \cdot 10^{-6}$ F/km, $L_e = 0.01978$ H, $L_0 = 23.886 \cdot 10^{-4}$ H/km, $C_0 = 0.35 \cdot 10^{-6}$ F/km, $L_{e0} = 0.24863$ H. These parameters are characteristic for the 35 kV cable IPZ013 (used in this case);
- the refraction and reflection of the traveling waves with velocity v = 83074.1 km/s (calculated using equation (3)), along the 2.163 km cable causes the frequency value of 9601.7 Hz (calculated using equation (5));
- the refraction and reflection of the traveling waves (zero component), with velocity v_0 = 34585.5 km/s (calculated using equation (4)) along the 2.163 km cable causes the frequency value of 3997.4 Hz (calculated using equation (6));
- the frequency of 7324.2 Hz occurs only at the start of the transient process (at first ms), before the circuit breaker contacts of different phases are closed, and it is the consequence of dissipations of the circuit breaker's switching moments in the line energization process. The frequency is not obtained by calculation, but by applying of the EMD method, as it is presented in Table I.

C. Deenergization of an unloaded 10 kV overhead transmission line

The analysis of the voltage signal, presented in Fig. 12, obtained by deenergization of an unloaded 10 kV overhead transmission line, with a multiple appearance of the arc between the circuit breaker contacts, was performed by the EMD method (Fig. 23 and Fig. 24). Fig. 23 presents the voltage signal, obtained by deenergization of the unloaded 10 kV overhead transmission line, decomposed into the intrinsic mode functions. The evaluation of the frequencies which were extracted from the decomposed voltage signal is presented in Fig. 24. The same signal was analyzed by a direct application of the STFT method, as presented in Fig. 25. The obtained results are presented in Table IV.

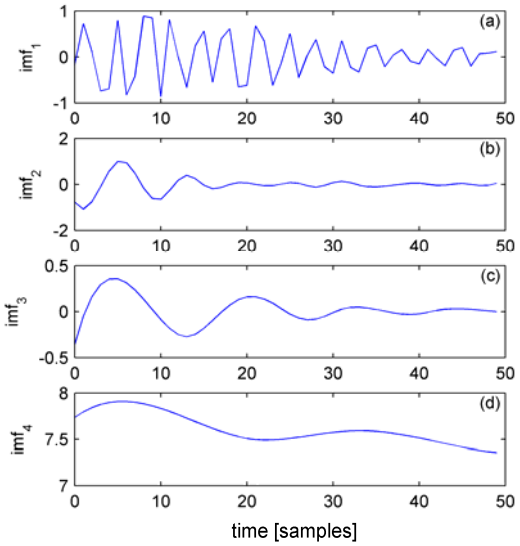

Figure 23. Voltage signal obtained at phase A by deenergization of an unloaded 10 kV overhead line, decomposed into intrinsic mode functions

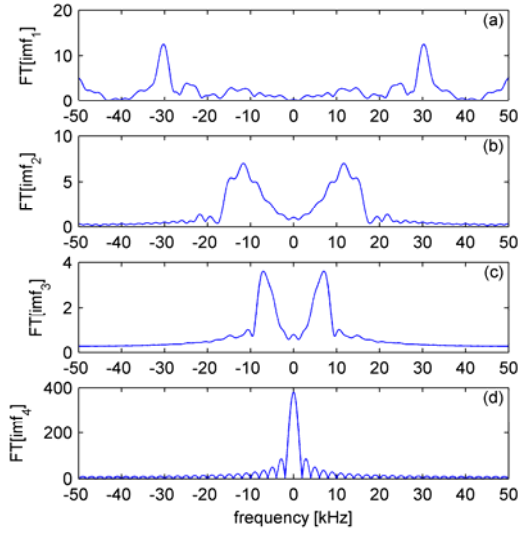

Figure 24. The evaluation of intrinsic mode function frequencies of the voltage signal obtained at phase A by deenergization of an unloaded 10 kV overhead line

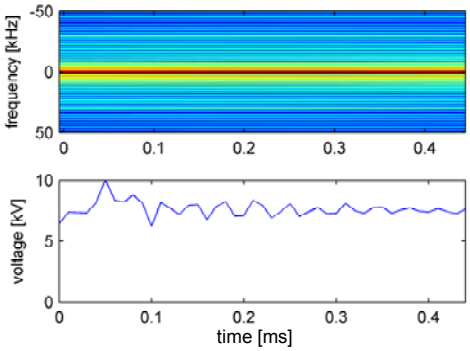

Figure 25. STFT analysis of the voltage signal obtained at phase A by deenergization of an unloaded 10 kV overhead line

TABLE IV FREQUENCIES OBTAINED BY THE EMD AND STFT METHODS COMPARED WITH THE CALCULATED VALUES FOR DEENERGIZATION OF AN UNLOADED 10 KV OVERHEAD LINE

Calculated frequency	EMD		STFT	
	Frequency	Error	Frequency	Error
6859 Hz	7050 Hz	2.78 %	2000 Hz	70.84 %
11460 Hz	11670 Hz	1.83 %	-	-
11741 Hz	-	-	-	-
14910.7 Hz	14540 Hz	2.48 %	-	-
	30272 Hz	-	29370 Hz	-

For the voltage signal obtained by an unloaded 10 kV overhead transmission line deenergization, the EMD method also provides very accurate results. Three out of four calculated values of the frequencies are extracted, with the error of 1.83 – 2.78%. The occurrence of a 30272 Hz frequency is also noted, which is the consequence of the circuit breaker's structural characteristics. In this case, by direct application of the STFT method, only one frequency value of 29370 Hz has been extracted.

The noted frequency values can be explained in the following way: the natural frequencies for the analyzed system are 11741 Hz and 6859 Hz; the refraction and reflection of the traveling waves with velocity v = 286285.6 km/s along the 4.8 km overhead line causes the frequency value of 14910.7 Hz; the refraction and reflection of the traveling waves (zero component), with velocity v_0 = 220032 km/s along the 4.8 km overhead line causes the frequency value of 11460 Hz. These values were obtained using equations (3)-(8), with the following input parameters: L= 1.226·10^{-3} H/km, C= 9.952·10^{-9} F/km, L_e= 0.000908 H, L_0= 4.19·10^{-3} H/km, C_0= 4.93·10^{-9} F/km, L_{e0}= 0.01272 H. Also, it should be mentioned the appearance of a frequency of 30272 Hz (see Table IV), which is detected by EMD method, and which is a result of the structural characteristics of the circuit breaker.

D. Energization of an unloaded 10 kV underground cable

The voltage signal presented in Fig. 13, which was obtained by energization of the unloaded 10 kV underground cable, was analyzed in a same manner as in a case given in the subsection IV.A. The signal decomposition into intrinsic mode functions is presented in Fig. 26, whereas Fourier transforms of the obtained IMFs are given in Fig. 27.

The same voltage signal, from which the 50 Hz sine component and the direct exponential component were removed, was also analyzed by the EMD method. Fig. 28 presents the voltage signal, decomposed into intrinsic mode functions. The evaluation of frequencies extracted from the decomposed voltage signal is presented in Fig 29.

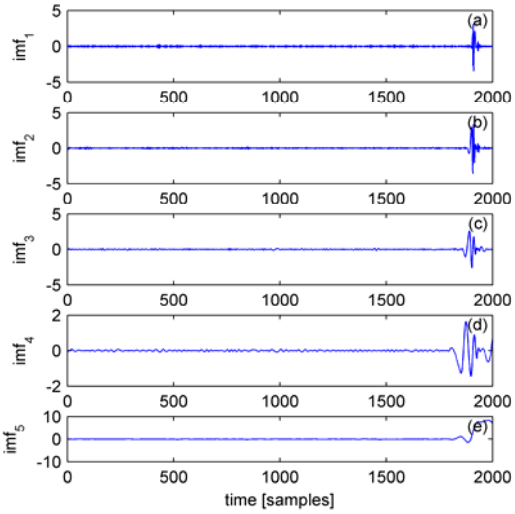

Figure 26. Voltage signal obtained at phase A by energization of the unloaded 10 kV underground cable, decomposed into IMFs.

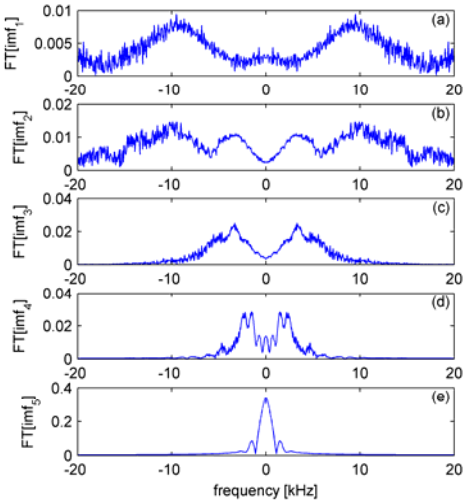

Figure 27. The evaluation of IMF frequencies of the voltage signal obtained at phase A by energization of an unloaded 10 kV underground cable

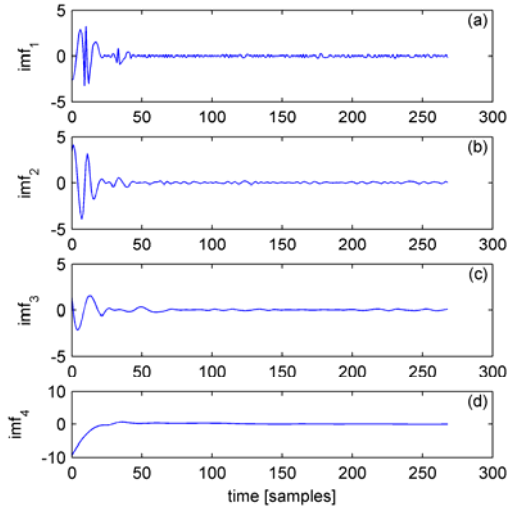

Figure 28. Voltage signal obtained at phase A by energization of the unloaded 10 kV underground cable, decomposed into IMFs (after the removal of the 50 Hz sine component and the direct exponential component)

Results obtained by the performed analysis were compared to the frequency values calculated by equations (5)-(8) and presented in Table V.

The signal was also analyzed by a direct application of

the STFT method, and the results are presented in Fig. 30, Fig. 31, and Table VI.

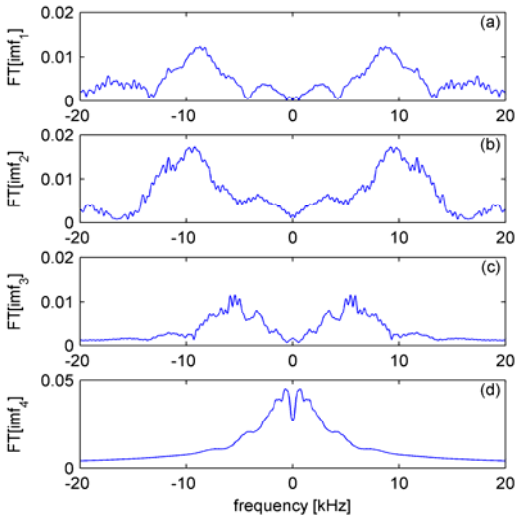

Figure 29. The evaluation of IMF frequencies of the voltage signal obtained at phase A by energization of an unloaded 10 kV underground cable (after the removal of the 50 Hz sine component and the direct exponential component)

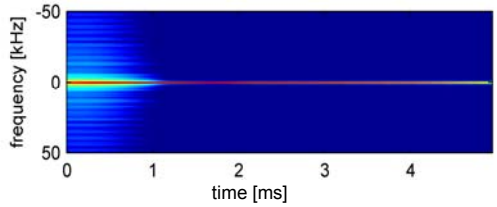

Figure 30. STFT analysis of the voltage signal obtained at phase A by energization of an unloaded 10 kV underground cable

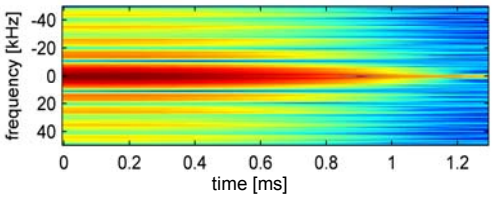

Figure 31. STFT analysis of the voltage signal obtained at phase A by energization of an unloaded 10 kV underground cable (after the removal of the 50 Hz sine component and the direct exponential component)

TABLE V FREQUENCIES OBTAINED BY EMD METHOD: DIRECTLY (EMD1); AFTER THE REMOVAL OF THE 50 HZ SINE COMPONENT AND THE DIRECT EXPONENTIAL COMPONENT (EMD2); COMPARED WITH THE CALCULATED VALUES FOR ENERGIZATION OF UNLOADED 10 KV UNDERGROUND CABLE

Calculated frequency	EMD 1		EMD 2	
	Frequency	Error	Frequency	Error
754Hz	683 Hz	9.32 %	707 Hz	6.23 %
1344 Hz	1464.9 Hz	8.95 %	1264.9 Hz	5.53%
2118 Hz	2197.2 Hz	3.74 %	2148.43 Hz	1.43 %
3385 Hz	3320.31 Hz	1.91 %	3471.95 Hz	0.97%
	9521.5 Hz		9521.5 Hz	

TABLE VI FREQUENCIES OBTAINED BY THE STFT METHOD: DIRECTLY (STFT1); AFTER THE REMOVAL OF THE 50 HZ SINE COMPONENT AND THE DIRECT EXPONENTIAL COMPONENT (STFT2); COMPARED WITH THE CALCULATED VALUES FOR ENERGIZATION OF UNLOADED 10 KV UNDERGROUND CABLE

Calculated frequency	STFT 1		STFT 2	
	Frequency	Error	Frequency	Error
754Hz	802 Hz	5.57 %	772	2.45 %
1344 Hz	1398 Hz	6.89 %	1560	16.07 %
2118 Hz	-	-	-	-
3385 Hz	-	-	-	-
			8950	

The comparison between the results of the analysis of the voltage signal obtained by the unloaded 10 kV underground cable energization and the calculated ones shows that results obtained by the EMD method are very close to the calculated values, especially when removal of the 50 Hz sine component and the direct exponential component from the original signal has been performed. In this case, all calculated values of the frequencies are extracted, with the error of 0.97-6.23%. The maximum error value, which corresponds to the minimum expected frequency of 754 Hz, is 6.23%. By the STFT, two out of four calculated values of the frequencies are extracted, with the error of 2.45-16.07%.

Using equations (3)-(8) and the following input parameters: L= $3.822 \cdot 10^{-4}$ H/km, C= $0.46 \cdot 10^{-6}$ F/km, L_e= 0.00114 H, L_0= $44.58 \cdot 10^{-4}$ H/km, C_0= $0.25 \cdot 10^{-6}$ F/km, L_{e0}= 0.0196 H, the calculated frequency values were obtained. These values, as well as the extracted frequency values can be explained in the following manner:

- the values of natural frequencies for the analyzed system are 2118 Hz and 754 Hz;
- the refraction and reflection of the traveling waves with velocity v = 75418.12 km/s along the 5.57 km cable causes the frequency value of 3385 Hz;
- the refraction and reflection of the traveling waves (zero component), with velocity v_0 = 29372 km/s along the 5.57 km cable causes the frequency value of 1344 Hz;
- the frequency of 9521.5 Hz occurs only at the start of the transient process (at first ms), before the circuit breaker contacts of different phases are closed, and it is the consequence of dissipations of the circuit breaker's switching moments in the line energization process. The frequency value is obtained by EMD method (Table V).

V. CONCLUSION

The increasing importance of power quality imposes the need for additional analysis that was not characteristic of traditional monopolistic power systems. This paper has shown that switching overvoltages have to be analyzed not only from the aspect of amplitude, but also from the aspect of the existing harmonics in the structure of the harmonic spectrum. For the purposes of harmonic decomposition it has been shown that the EMD method is extremely reliable and that its application, with high precision, can get the harmonic spectrum of various surge waves. This information is important for detecting the location of the overvoltages occurrence and for a speedy intervention in order to stabilize the voltage conditions and restore power quality to the required level.

ACKNOWLEDGMENT

The authors would like to thank Prof. Ilija Vujošević for providing an experimental signals used in this paper.

REFERENCES

[1] P. Caramia, G. Carpinelli, and P. Verde, "Power Quality Indices in Liberalized Market", Wiley, Chichester, U.K, 2009. DOI:10.1002/9780470994405.ch1

[2] E. Fuchs, M. Masoum, "Power Quality in Power Systems and Electrical Machines", Elsevier Academic Press, Burlington, 2008.

[3] J. M. Knezevic, V. A. Katic, "The hybrid method for on-line harmonic analysis", Advances in Electrical and Computer Engineering, Vol. 11, No. 3, 2011, pp. 29 - 34. DOI:10.4316/AECE.2011.03005

[4] A. Miron, M. D. Chindris, A. C. Cziker, "Software Tool for Real-Time Power Quality Analysis," Advanced in Electrical and Computer Engineering, Vol. 13, No. 4, 2013, pp. 125-132. DOI:10.4316/AECE.2013.04021

[5] V. C. Nikolaidis, I. Milis, G. Rizopoulos, "Transient Phenomena Analysis and Protection Evaluation in an Industrial Power Systems", VII MedPower 2010 Conf., Nov. 2010, Agia Napa, Cyprus, pp. 1-10. DOI:10.1049/cp.2010.0928

[6] M. Davila, J. L. Naredo, P. Moreno, A. Ramirez, "Practical Implementation of a Transmission Line Model for Transient Analysis Considering Corona and Skin Effects", IEEE Bologna Power Tech Conference, 2003, Bologna, Italy.DOI:10.1109/PTC2003.1304641

[7] S. Škuletić, S. Vujosević, "Possibilities for an analysis of switching overvoltages due to three-phase faults tripping with a discrete method", 35th UPEC 2000 Conf., Sept. 2000, Belfast, NIrl., P. No. 2.

[8] S. Škuletić, S. Vujosević, "Analysis of switching overvoltages originated by line energizing in simple and complex systems", 36th UPEC 2001 Conf., September 2001, Swansea, UK, Paper No. 413.

[9] A.I. Ramirez, A. Semlyen, R. Iravani, "Modeling Nonuniform Transmission Lines for Time Domain Simulation of Electromagnetic Transients", IEEE Trans, on Power Delivery, Vol. 18, No.3, Jully 2003, pp. 968-974.DOI10.1109/TPWRD.2003.813877

[10] S. Vujosević, S. Škuletić, "Energization of an unloaded three-phase transmission line with consideration of frequency dependent parameters, corona effects and dissipations of circuit breaker switching moments", 40th UPEC 2005 Conference, Cork, UK, September 2005, paper No.95.

[11] Y.H. Gu, M.H.J. Bollen, "Time-Frequency and Time-scale Domain Analysis of Voltage Disturbances", IEEE Transactions on Power Delivery, Vol. 14, No. 4, October 2000, pp. 1279-1284.DOI:10.1109/61.891515

[12] N. E. Huang, Z. Shen, S. R. Long, M. C. Wu, H. H. Shih, Q. Zheng, N-C. Yen, C. C. Tung, and H. H. Liu, "The Empirical Mode Decomposition and the Hilbert-Spectrum for Nonlinear and Non-stationary Time Series Analysis", Proc. R. Soc. London, Vol. 454, No. 1971, 1998, pp. 903-995.DOI:10.1098/rspa.1998.0193

[13] Z. Lu, J. S. Smith, Q. H. Wu, J. Fitch, "Empirical Mode Decomposition For Power Quality Monitoring", 2005 IEEE/PES Conference, 2005, Dalian, pp. 1-5.DOI:10.1109/TDC.2005.1546916

[14] S. Vujosevic, J. Radovic, M. Dakovic, "EMD And STFT Signal Processing Methods Used for the Analysis of the Energisation of an Unloaded Three-Phase Transmission Line", 44th UPEC 2009 Conference, 2009, Glasgow, Schotland.

[15] M. Ortis, S. Valero, A. Gabaldon, "Transient Power and Quality Events Analysed Using Hilbert Transforms", Journal of Energy and Power Engineering, Vol. 6, 2012, pp 230-239. DOI: 10.1007/978-3-642-35314-7_18

[16] A. Elmitwally, S. Mahmoud, M. H. Abdel-Rahman, "Fault Identification of Overhead Transmission Lines Terminated with Underground Cables", 14th International Middle East Power Systems Conference, December 2010, Cairo, Egypt, Paper ID 202.

[17] B.K. Panigrahi, V. R. Pandi, "Oprimal feature for classification of power quality disturbances using wavelet packet-based fuzzy k-nearest neighbour algorithm", IET Generation, Transimission and Distribution, Vol. 3, No. 3, 2009, pp. 296-306. DOI: 10.1049/iet-gtd:20080190

[18] C.F. Norman, J.Y.C. Chan, W.-Hong Lau, J. T.Y. Poon, and L.L. Lai, Fellow, "Real-Time Power Quality Monitoring With Hybrid Sinusoidal and Lifting Wavelet Compression Algorithm", IEEE Trans. On Power Delivery, Vol. 27, No. 4, 2012, pp. 1718-1726. DOI:10.1109/TPWRD.2012.2201510

[19] J. Barros, R. I. Diego, M. de Apraiz,"Application of wavelets in electric power quality: Voltage events", Electrical Power System Research, Vol. 88, 2012, pp.130-136.DOI:10.1016/j.epsr.2012.02.009

[20] C. Y. Lee, Y.-X. Shen, "Optimal feature Selection for Power Quality Didsturbances Classification", IEEE Trans. On Power Delivery, Vol. 26, No. 4, 2011, pp. 2342-2351.DOI:10.1109/TPWRD.2011.2149542

[21] S. Avdakovic, A. Nuhanovic, M. Kusljugic, M. Music, "Wavlet transform application in power system dynamic, Electrical Power System Research, Vol. 83, 2012, pp. 237-245. DOI:10.1016/j.epsr.2010.11.031

[22] LJ. Stanković, M. Daković, T. Thayaparan, "Time-Frequency Signal Analysis with Applications", Artech House, Boston, USA, 2013.

[23] V. Maier, S. G. Pavel, C. D. Maier, I. Birou, "Correct Application of the Discrete Fourier Transform in Harmonics," Advanced in Electrical and Computer Engineering, Vol. 8, No. 1, 2009, pp. 26-30. DOI:10.4316/aece.2008.01005

[24] I. W. C. Lee, P. K. Dash, "S-transform-based intelligent system for classification of power quality disturbance signals", IEEE Trans. on Industrial Electronics, Vol. 50, No. 4, 2003, pp. 800-805. DOI10.1109/TIE.2003.814991

[25] L. Bin, S. H. Chun, "Research on Fault Line Detecting Based on Empirical Mode Decomposition (EMD) in Resonant Grounded Systems", APPEEC 2009 Conference, March 2009, Wuhan, pp. 1-5. DOI:10.1109/APPEEC.2009.4918686

[26] B. Bjelica, M. Daković, LJ. Stanković, T. Thayaparan, "Complex Empirical Decomposition method in radar signal processing," 2012 MECO Conference, June 2012, Bar, Montenegro, pp.88-91